
A Simple and Effective Reinforcement Learning Method for Text-to-Image Diffusion Fine-tuning

Shashank Gupta^{* 1 2} Chaitanya Ahuja¹ Tsung-Yu Lin¹ Sreya Dutta Roy¹ Harrie Oosterhuis³
Maarten de Rijke² Satya Narayan Shukla¹

Abstract

Reinforcement learning (RL)-based fine-tuning has emerged as a powerful approach for aligning diffusion models with black-box objectives. Proximal policy optimization (PPO) is the most popular choice of method for policy optimization. While effective in terms of performance, PPO is highly sensitive to hyper-parameters and involves substantial computational overhead. REINFORCE, on the other hand, mitigates some computational complexities such as high memory overhead and sensitive hyper-parameter tuning, but has suboptimal performance due to high-variance and sample inefficiency. While the variance of the REINFORCE can be reduced by sampling multiple actions per input prompt and using a baseline correction term, it still suffers from sample inefficiency. To address these challenges, we systematically analyze the *efficiency-effectiveness* trade-off between REINFORCE and PPO, and propose leave-one-out PPO (LOOP), a novel RL for diffusion fine-tuning method. LOOP combines variance reduction techniques from REINFORCE, such as sampling multiple actions per input prompt and a baseline correction term, with the robustness and sample efficiency of PPO via clipping and importance sampling. Our results demonstrate that LOOP effectively improves diffusion models on various black-box objectives, and achieves a better balance between computational efficiency and performance.

1. Introduction

Diffusion models have emerged as a powerful tool for generative modeling (Sohl-Dickstein et al., 2015; Ho et al., 2020),

^{*}Work done during an internship at Meta ¹Meta ²University of Amsterdam, The Netherlands ³Radboud University, Nijmegen, The Netherlands. Correspondence to: Shashank Gupta <s.gupta2@uva.nl>, Satya Narayan Shukla <satyan-shukla@meta.com>.

with a strong capacity to model complex data distributions from various modalities, like images (Rombach et al., 2022), text (Austin et al., 2021), natural molecules (Xu et al., 2023), and videos (Blattmann et al., 2023).

Diffusion models are typically pre-trained on a large-scale dataset, such that they can subsequently generate samples from the same data distribution. The training objective typically involves maximizing the data distribution likelihood. This pre-training stage helps generate high-quality samples from the model. However, some applications might require optimizing a custom reward function, for example, optimizing for generating aesthetically pleasing images (Xu et al., 2024), semantic alignment of image-text pairs based on human feedback (Schuhmann et al., 2022), or generating molecules with specific properties (Wang et al., 2024).

To optimize for such black-box objectives, RL-based fine-tuning has been successfully applied to diffusion models (Fan et al., 2024; Black et al., 2023; Wallace et al., 2024; Li et al., 2024; Gu et al., 2024). For RL-based fine-tuning, the reverse diffusion process is treated as a Markov decision process (MDP), wherein prompts are treated as part of the input state, the generated image at each time-step is mapped to an action, which receives a reward from a fixed reward model (environment in standard MDP), and finally the diffusion model is treated as a policy, which we optimize to maximize rewards. For optimization, typically PPO is applied (Fan et al., 2024; Black et al., 2023). In applications where getting a reward model is infeasible or undesirable, “RL-free” fine-tuning (typically offline) can also be applied (Wallace et al., 2024; Yang et al., 2024). For this work, we only focus on diffusion model finetuning using “online” RL methods, specifically PPO (Schulman et al., 2017).

An advantage of PPO is that it removes the incentive for the new policy to deviate too much from the previous reference policy, via importance sampling and clipping operation (Schulman et al., 2017). While effective, PPO can have significant computational overhead. In practice, RL fine-tuning for diffusion models via PPO requires concurrently loading three models in memory: (i) The **reference policy**: The base policy, which is usually initialized with

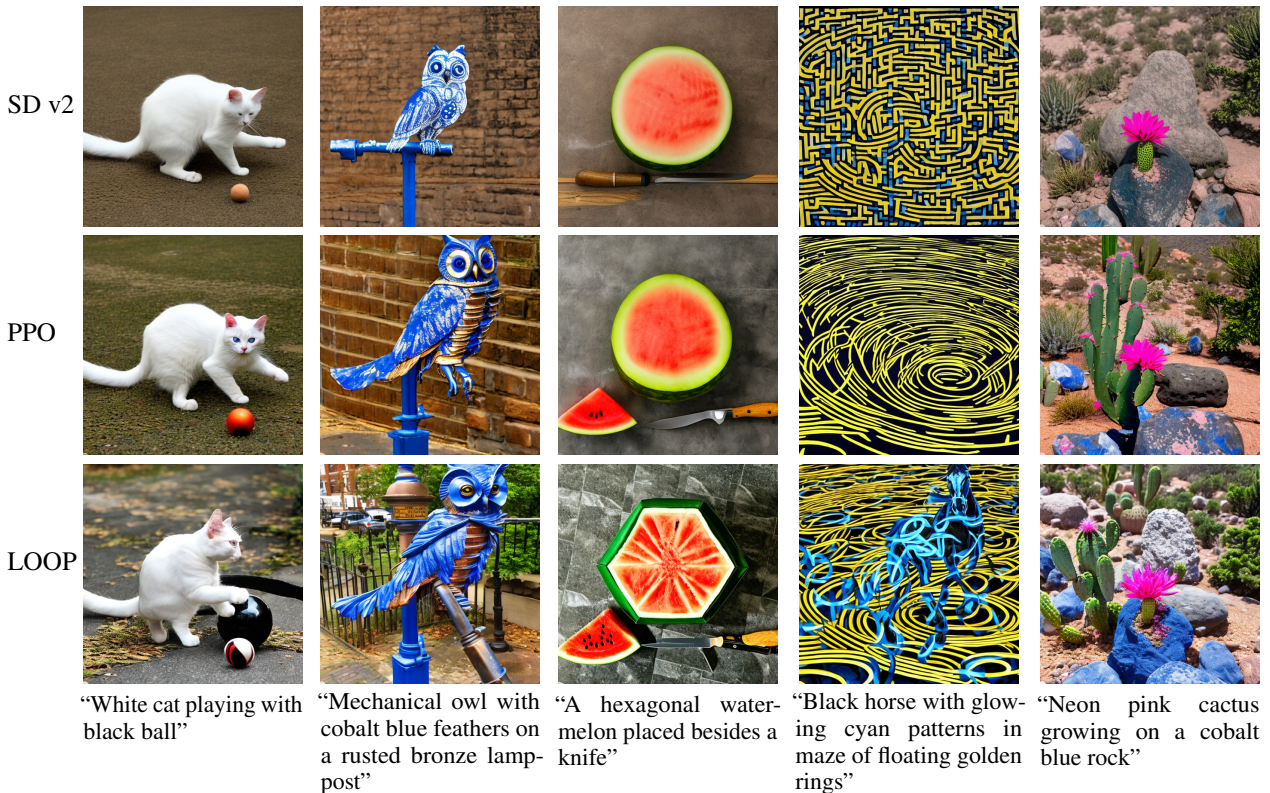


Figure 1. **LOOP improves attribute binding.** Qualitative examples presented from images generated via Stable Diffusion (SD) 2.0 (first row), PPO (second row), and LOOP $k = 4$ (third row). In the first prompt, SD and PPO both fail to bind the *color black* with the *ball* in the image, whereas LOOP binds the color black to the ball. In the second example, SD and PPO fail to generate *rusted bronze color* lamp-post, whereas LOOP manages to do that. In the third image, SD and PPO fail to bind the *shape hexagon* to the watermelon, whereas LOOP manages so. In the fourth example, SD and PPO fail to generate the *black horse* with flowing cyan patterns, whereas LOOP generates the horse with the correct color attribute. Finally, in the last image, SD and PPO fail to bind *cobalt blue* color to the rock, whereas LOOP binds that successfully.

the pre-trained diffusion model. (ii) The **current policy**: The policy that is RL fine-tuned, and also initialized with the pre-trained diffusion model. (iii) The **reward model**: Typically, a large vision-language model, trained via supervised fine-tuning objective (Lee et al., 2023), which assigns a scalar reward to the final generated image during the online optimization stage. This can result in a considerable computational burden, given that each policy can potentially have millions of parameters. In addition to computational overhead, PPO is also known to be sensitive to hyper-parameters (Engstrom et al., 2019; Zheng et al., 2023; Huang et al., 2024).

Simpler approaches, like REINFORCE (Williams, 1992) avoid such complexities, and could theoretically be more efficient. However, in practice, they often suffer from high variance and instability. Recently, a variant of REINFORCE: reinforce leave-one-out (RLOO) (Kool et al., 2019) was proposed which samples multiple sequences per input prompt, and a baseline correction term to reduce the variance, however, it still suffers from sample inefficiency.

This raises a fundamental question about **efficiency-effectiveness** trade-off in RL-based diffusion fine-tuning. In this work, first we systematically explore this trade-off between *efficiency* – a lower computational cost, and reduced implementation complexity (i.e., fewer hyper-parameters) – and *effectiveness* – stable training, and final performance. We compare a simple REINFORCE approach with the standard PPO framework, demonstrating that while REINFORCE greatly reduces computational complexity, it comes at the cost of reduced performance.

Motivated by this finding, we propose a novel RL for diffusion fine-tuning method, LOOP, which combines the best of the both worlds. To reduce the variance during policy optimization, LOOP leverages multiple actions (diffusion trajectories) and a (REINFORCE) baseline correction term per input prompt. To maintain the stability and robustness of PPO, LOOP leverages clipping and importance sampling. We note that LOOP was discovered independently in the context of long-horizon interactive LLM agent training by Chen et al. (2025).

We choose the text-to-image compositionality benchmark (T2I-CompBench; Huang et al., 2023) as our primary evaluation benchmark. Text-to-image models often fail to satisfy an essential reasoning ability of attribute binding, i.e., the generated image often fails to *bind* certain *attributes* specified in the instruction prompt (Huang et al., 2023; Ramesh et al., 2022; Fu & Cheng, 2024). As illustrated in Figure 1, LOOP outperforms previous diffusion methods on attribute binding. As attribute binding is a key skill necessary for real-world applications, we choose the T2I-CompBench benchmark alongside two other common tasks: aesthetic image generation and image-text semantic alignment.

To summarize, our main contributions are as follows:

PPO vs. REINFORCE efficiency-effectiveness trade-off.

We systematically study how design elements like clipping, reference policy, value function in PPO compare to a simple REINFORCE method, highlighting the efficiency-effectiveness trade-off in diffusion fine-tuning. To the best of our knowledge, we are the first ones to present such a systematic study, highlighting the trade-offs in diffusion fine-tuning.

Introducing LOOP. We propose LOOP, a novel RL for diffusion fine-tuning method combining the best of REINFORCE and PPO. LOOP leverages multiple diffusion trajectories and a REINFORCE baseline correction term for variance reduction, as well as clipping and importance sampling from PPO for robustness and sample efficiency.

Empirical validation. To validate our claims empirically, we conduct experiments on the T2I-CompBench benchmark image compositionality benchmark. The benchmark evaluates the attribute binding capabilities of the text-to-image generative models and shows that LOOP succeeds where previous text-to-image generative models often fail. We also evaluate LOOP on two common objectives from RL for diffusion literature: image aesthetic, and text-image semantic alignment (Black et al., 2023).

2. Background and Related Work

2.1. Diffusion Models

We focus on denoising diffusion probabilistic models (DDPM) as the base model for text-to-image generative modeling (Ho et al., 2020; Sohl-Dickstein et al., 2015). Briefly, given a conditioning context variable \mathbf{c} (text prompt in our case), and the data sample \mathbf{x}_0 , DDPM models $p(\mathbf{x}_0 | \mathbf{c})$ via a Markov chain of length T , with the following dynamics:

$$p_\theta(\mathbf{x}_{0:T} | \mathbf{c}) = p(\mathbf{x}_T | \mathbf{c}) \prod_{t=1}^T p_\theta(\mathbf{x}_{t-1} | \mathbf{x}_t, \mathbf{c}). \quad (1)$$

Image generation in diffusion model is achieved via the following ancestral sampling scheme, which is a reverse diffusion process:

$$\begin{aligned} \mathbf{x}_T &\sim \mathcal{N}(\mathbf{0}, \mathbf{I}), \\ \mathbf{x}_t &\sim N(\mathbf{x}_t | \mu_\theta(\mathbf{x}_t, \mathbf{c}, t), \sigma_\theta^2 I), \forall t \in [0, T-1], \end{aligned} \quad (2)$$

where the distribution at time-step t is assumed to be a multivariate normal distribution with the predicted mean $\mu_\theta(\mathbf{x}_t, \mathbf{c}, t)$, and a constant variance.

2.2. Proximal Policy Optimization (PPO) for RL

PPO was introduced for optimizing a policy with the objective of maximizing the overall reward in the RL paradigm. PPO removes the incentive for the current policy π_t to diverge from the previous policy π_{t-1} outside the range $[1 - \epsilon, 1 + \epsilon]$, where ϵ is a hyper-parameter. As long as the subsequent policies are closer to each other in the action space, the monotonic policy improvement bound guarantees a monotonic improvement in the policy’s performance as the optimization progresses. This property justifies the clipping term in the mathematical formulation of the PPO objective function (Schulman, 2015; Achiam et al., 2017; Queeney et al., 2021). Formally, PPO the objective function is:

$$J(\theta) = \mathbb{E} \left[\min \left(r_t(\theta) \hat{A}_t, \text{clip} \left(r_t(\theta), 1 - \epsilon, 1 + \epsilon \right) \hat{A}_t \right) \right], \quad (3)$$

where $r_t(\theta) = \frac{\pi_t(a|c)}{\pi_{t-1}(a|c)}$ is the importance sampling ratio between the current policy $\pi_t(a | c)$ and the previous reference policy $\pi_{t-1}(a | c)$, \hat{A}_t is the advantage function (Sutton & Barto, 2018), and the clip operator restricts the importance sampling ratio in the range $[1 - \epsilon, 1 + \epsilon]$.

2.3. RL for Text-to-Image Diffusion Models

The diffusion process can be viewed as an MDP $(\mathcal{S}, \mathcal{A}, \mathcal{P}, \mathcal{R}, \rho_0)$, where \mathcal{S} is the state space, \mathcal{A} is the action space, \mathcal{P} is the state transition kernel, \mathcal{R} is the reward function, and ρ_0 is the distribution of initial state \mathbf{s}_0 . In the context of text-to-image diffusion models, the MDP is defined as:

$$\begin{aligned} \mathbf{s}_t &= (\mathbf{c}, t, \mathbf{x}_t), \quad \pi_\theta(\mathbf{a}_t | \mathbf{s}_t) = p_\theta(\mathbf{x}_{t-1} | \mathbf{x}_t, \mathbf{c}), \\ \mathcal{P}(\mathbf{s}_{t+1} | \mathbf{s}_t, \mathbf{a}_t) &= \delta(\mathbf{c}, \mathbf{a}_t), \quad \mathbf{a}_t = \mathbf{x}_{t-1}, \\ \rho_0(\mathbf{s}_0) &= (p(\mathbf{c}), \delta_T, \mathcal{N}(\mathbf{0}, \mathbf{I})), \\ \mathcal{R}(\mathbf{s}_t, \mathbf{a}_t) &= \begin{cases} r(\mathbf{x}_0, \mathbf{c}) & \text{if } t = 0, \\ 0 & \text{otherwise.} \end{cases} \end{aligned} \quad (4)$$

The input state \mathbf{s}_t is defined in terms of the context (prompt features), sampled image at the given time-step t . The policy π_θ is the diffusion model itself. The state transition kernel is a dirac delta function δ with the current sampled action \mathbf{x}_t as the input. The reward is assigned only at the last step in the reverse diffusion process, when the final image is generated. The initial state ρ_0 corresponds to the last state in the forward diffusion process: \mathbf{x}_T .

2.4. PPO for Diffusion Fine-tuning

The objective function of RL fine-tuning for a diffusion policy π_θ can be defined as follows:

$$\begin{aligned} J_\theta(\pi) &= \mathbb{E}_{\tau \sim p(\tau | \pi_\theta)} \left[\sum_{t=0}^T \mathcal{R}(\mathbf{s}_t, \mathbf{a}_t) \right] \\ &= \mathbb{E}_{\tau \sim p(\tau | \pi_\theta)} [r(\mathbf{x}_0, \mathbf{c})], \end{aligned} \quad (5)$$

where the trajectory $\tau = \{\mathbf{x}_T, \mathbf{x}_{T-1}, \dots, \mathbf{x}_0\}$ refers to the reverse diffusion process (Eq. 1), and the total reward of the trajectory is the reward of the final generated image \mathbf{x}_0 (Eq. 4). We ignore the KL-regularized version of the equation, which is commonly applied in the RLHF for LLM literature (Zhong et al., 2024; Zeng et al., 2024; Rafailov et al., 2024), and proposed by Fan et al. (2024) in the context of RL for diffusion models. As shown by Black et al. (2023), adding the KL-regularization term makes no empirical difference in terms of the final performance. The PPO objective is given as:

$$\begin{aligned} J_\theta^{\text{PPO}}(\pi) &= \\ &\mathbb{E} \left[\sum_{t=0}^T \text{clip} \left(\frac{\pi_\theta(\mathbf{x}_{t-1} | \mathbf{x}_t, \mathbf{c})}{\pi_{\text{old}}(\mathbf{x}_{t-1} | \mathbf{x}_t, \mathbf{c})}, 1 - \epsilon, 1 + \epsilon \right) r(\mathbf{x}_0, \mathbf{c}) \right], \end{aligned} \quad (6)$$

where the clipping operation removes the incentive for the new policy π_θ to differ from the previous round policy π_{old} (Schulman et al., 2017; Black et al., 2023).

3. REINFORCE vs. PPO:

An Efficiency-Effectiveness Trade-Off

In this section, we explore the efficiency-effectiveness trade-off between two prominent reinforcement learning methods for diffusion fine-tuning: REINFORCE and PPO. Understanding this trade-off is crucial for selecting the appropriate algorithm given constraints on computational resources and desired performance outcomes.

In the context of text-to-image diffusion models, we aim to optimize the policy π to maximize the expected reward $\mathcal{R}(x_{0:T}, c) = r(x_0, c)$. Our objective function is defined as:

$$J_\theta(\pi) = \mathbb{E}_{c \sim p(C), x_{0:T} \sim p_\theta(x_{0:T} | c)} [r(x_0, c)]. \quad (7)$$

REINFORCE for gradient calculation. For optimizing this objective, the REINFORCE policy gradient (also known as score function (SF)) (Williams, 1992) provides the following gradient estimate:

$$\begin{aligned} \nabla_\theta J_\theta^{\text{SF}}(\pi) &= \mathbb{E}_{\mathbf{x}_{0:T}} \left[\nabla_\theta \log \left(\prod_{t=1}^T p_\theta(\mathbf{x}_{t-1} | \mathbf{x}_t, \mathbf{c}) \right) r(\mathbf{x}_0, \mathbf{c}) \right] \\ &= \mathbb{E}_{\mathbf{x}_{0:T}} \left[\sum_{t=0}^T \nabla_\theta \log p_\theta(\mathbf{x}_{t-1} | \mathbf{x}_t, \mathbf{c}) r(\mathbf{x}_0, \mathbf{c}) \right], \end{aligned} \quad (8)$$

where the second step follows from the reverse diffusion policy decomposition (Eq. 1).

In practice, a batch of trajectories is sampled from the reverse diffusion distribution, i.e., $\mathbf{x}_{0:T} \sim p_\theta(\mathbf{x}_{0:T})$, and a Monte-Carlo estimate of the REINFORCE policy gradient (Eq. 8) is calculated for the model update.

REINFORCE with baseline correction. To reduce variance of the REINFORCE estimator, a common trick is to subtract a constant baseline correction term from the reward function (Greensmith et al., 2004; Mohamed et al., 2020):

$$\begin{aligned} \nabla_\theta J_\theta^{\text{SFB}}(\pi) &= \\ &\mathbb{E} \left[\sum_{t=0}^T \nabla_\theta \log p_\theta(\mathbf{x}_{t-1} | \mathbf{x}_t, \mathbf{c}) (r(\mathbf{x}_0, \mathbf{c}) - b_t) \right]. \end{aligned} \quad (9)$$

REINFORCE Leave-one-out (RLOO). To further reduce the variance of the REINFORCE estimator, RLOO samples K diffusion trajectories per prompt ($\{\mathbf{x}_{0:T}^k\} \sim \pi(\cdot | \mathbf{c})$), for a better Monte-Carlo estimate of the expectation (Kool et al., 2019; Ahmadian et al., 2024). The RLOO estimator is:

$$\begin{aligned} \nabla_\theta J_\theta^{\text{RLOO}}(\pi) &= \\ &\mathbb{E} \left[K^{-1} \sum_{k=0}^K \sum_{t=0}^T \nabla_\theta \log p_\theta(\mathbf{x}_{t-1}^k | \mathbf{x}_t^k, \mathbf{c}) (r(\mathbf{x}_0^k, \mathbf{c}) - b_t) \right]. \end{aligned} \quad (10)$$

However, REINFORCE-based estimators have a significant disadvantage: they do not allow sample reuse (i.e., reusing trajectories collected from previous policies) due to a distribution shift between policy gradient updates during training. Sampled trajectories can only be used once, prohibiting mini-batch updates. This makes it *sample inefficient*.

To allow for sample reuse, the importance sampling (IS) trick can be applied (Schulman, 2015; Owen, 2013):

$$J_\theta^{\text{IS}}(\pi) = \mathbb{E}_{c_t \sim p(C), a_t \sim \pi_{\text{old}}(a_t | c_t)} \left[\frac{\pi_\theta(a_t | c_t)}{\pi_{\text{old}}(a_t | c_t)} \mathcal{R}_t \right], \quad (11)$$

where π_θ is the *current* policy to be optimized, and π_{old} is the policy from the previous update round. With the IS trick, we can sample trajectories from the current policy in a batch, store it in a temporary buffer, and re-use them to apply mini-batch optimization (Schulman et al., 2017).

Motivation for PPO. With the IS trick, the samples from the old policy can be used to estimate the policy gradient under the current policy π_θ (Eq. 8) in a statistically unbiased fashion (Owen, 2013), i.e., in expectation the IS and REINFORCE gradients are equivalent (Eq. ??, Eq. 8). Thus, potentially, we can improve the sample efficiency of REINFORCE gradient estimation with IS.

While unbiased, the IS estimator can exhibit high variance (Owen, 2013). This high variance may lead to unstable

training dynamics. Additionally, significant divergence between the current policy π_θ and the previous policy π_{old} can result in the updated diffusion policy performing worse than the previous one (Schulman, 2015; Achiam et al., 2017). Next, we will prove this formally. We note that this result has previously been established by (Achiam et al., 2017) for the more general RL setting. In this work, we extend this finding to the context of diffusion model fine-tuning.

A key component of the proof relies on the distribution of states under the current policy, i.e., $d^\pi(s)$. In the case of diffusion models, the state transition kernel $P(s_{t+1} | s_t, a_t)$ is deterministic, because the next state consists of the action sampled from the previous state (Eq. 4), i.e., $P(s_{t+1} | s_t, a_t) = 1$. While the state transition kernel is deterministic, the distribution of states is stochastic, given that it depends on the action at time t , which is sampled from the policy (Eq. 4). We define the state distribution as:

Definition 1. Given the distribution over contexts $\mathbf{c} \sim p(\mathbf{C})$, the (deterministic) distribution over time $t = \delta(t)$, and the diffusion policy π , the state distribution at time t is:

$$p(\mathbf{s}_t | \pi) = p(\mathbf{c})\delta(t) \int \pi(\mathbf{x}_t | \mathbf{x}_{t+1}, \mathbf{c}, t) \pi(\mathbf{x}_{t+1} | \mathbf{c}, t) d\mathbf{x}_{t+1}.$$

Subsequently, the normalized discounted state visitation distribution can be defined as:

$$d^\pi(\mathbf{s}) = (1 - \gamma) \sum_{t=0}^{\infty} \gamma^t p(\mathbf{s}_t = \mathbf{s} | \pi). \quad (12)$$

The advantage function is defined as: $A^{\pi_k}(\mathbf{s}, \mathbf{a}) = Q^{\pi_k}(\mathbf{s}, \mathbf{a}) - V^{\pi_k}(\mathbf{s})$ (Sutton & Barto, 2018). Given this, the monotonic policy improvement bound can be derived:

Theorem 3.1. (Achiam et al., 2017) Consider a current policy π_k . For any future policy π , we have:

$$J(\pi) - J(\pi_k) \geq \frac{1}{1 - \gamma} \mathbb{E}_{(s,a) \sim d^{\pi_k}} \left[\frac{\pi(a | s)}{\pi_k(a | s)} A^{\pi_k}(s, a) \right] - \frac{2\gamma C^{\pi, \pi_k}}{(1 - \gamma)^2} \mathbb{E}_{s \sim d^{\pi_k}} [\text{TV}(\pi(\cdot | s), \pi_k(\cdot | s))],$$

where $C^{\pi, \pi_k} = \max_{s \in S} |\mathbb{E}_{a \sim \pi(\cdot | s)} [A^{\pi_k}(s, a)]|$ and $\text{TV}(\pi(\cdot | s), \pi_k(\cdot | s))$ represents the total variation distance between the policies $\pi(\cdot | s)$ and $\pi_k(\cdot | s)$.

A direct consequence of this theorem is that when optimizing a policy with the IS objective (Eq. 11), to guarantee that the new policy will improve upon the previous policy, the policies should not diverge too much. Therefore, we need to apply a constraint on the current policy. This can be achieved by applying the clipping operator in the PPO objective (Eq. 6) (Queeney et al., 2021; Achiam et al., 2017; Schulman et al., 2017; Gupta et al., 2024b).

This gives rise to an *efficiency-effectiveness trade-off* between REINFORCE and PPO. REINFORCE offers greater computational and implementation efficiency due to its simplicity, but it comes at the cost of lower sample efficiency and potential suboptimal performance. In contrast, PPO is more computationally demanding and involves more complex hyper-parameter tuning, yet it achieves higher performance and reliable policy improvements during training.

We note that a similar trade-off analysis was performed in the context of RL fine-tuning for large language models (LLM) (Ahmadian et al., 2024). However, their analysis was limited to an empirical study, whereas we present a theoretical analysis in addition to the empirical analysis. To the best of our knowledge, we are the first to conduct such a study for diffusion methods.

4. Method: Leave-One-Out PPO (LOOP) for Diffusion Fine-tuning

We demonstrated the importance of PPO in enhancing sample efficiency and achieving stable improvements during training for diffusion fine-tuning. Additionally, we showcased the RLOO method’s effectiveness in reducing the variance of the REINFORCE method. In this section, we introduce our proposed method, **LOOP**, a novel RL for diffusion fine-tuning method. We start with highlighting the potential high-variance in the PPO objective.

The expectation in the PPO loss (Eq. 6) is typically estimated by sampling a single trajectory for a given prompt c :

$$\sum_{t=0}^T \text{clip} \left(\frac{\pi_\theta(\mathbf{x}_{t-1} | \mathbf{x}_t, \mathbf{c})}{\pi_{\text{old}}(\mathbf{x}_{t-1} | \mathbf{x}_t, \mathbf{c})}, 1 - \epsilon, 1 + \epsilon \right) r(\mathbf{x}_0, \mathbf{c}), \quad (13)$$

where $\mathbf{x}_{0:T} \sim \pi_{\text{old}}$. Even though the single sample estimate is an unbiased Monte-Carlo approximation of the expectation, it has high-variance (Owen, 2013). Additionally, the IS term $\left(\frac{\pi_\theta(\mathbf{x}_{t-1} | \mathbf{x}_t, \mathbf{c})}{\pi_{\text{old}}(\mathbf{x}_{t-1} | \mathbf{x}_t, \mathbf{c})} \right)$ can also contribute to high-variance of the PPO objective (Swaminathan & Joachims, 2015; Xie et al., 2023). Both factors combined, can lead to high-variance, and unstable training of the PPO.

Taking inspiration from RLOO (Eq. 10), we sample K independent trajectories from the previous policy for a given prompt c , and apply a baseline correction term from each trajectory reward, to reduce the variance of the estimator:

$$\hat{J}_\theta^{\text{LOOP}}(\pi) = \frac{1}{K} \sum_{i=1}^K \left[\sum_{t=0}^T \text{clip} \left(\frac{\pi_\theta(\mathbf{x}_{t-1}^i | \mathbf{x}_t^i, c)}{\pi_{\text{old}}(\mathbf{x}_{t-1}^i | \mathbf{x}_t^i, c)}, 1 - \epsilon, 1 + \epsilon \right) \cdot (r(\mathbf{x}_0^i, \mathbf{c}) - b^i) \right], \quad (14)$$

where $\mathbf{x}_{0:T}^i \sim \pi_{\text{old}}, \forall i \in [1, K]$. The baseline correction term b^i reduces the variance of the gradient estimate, while

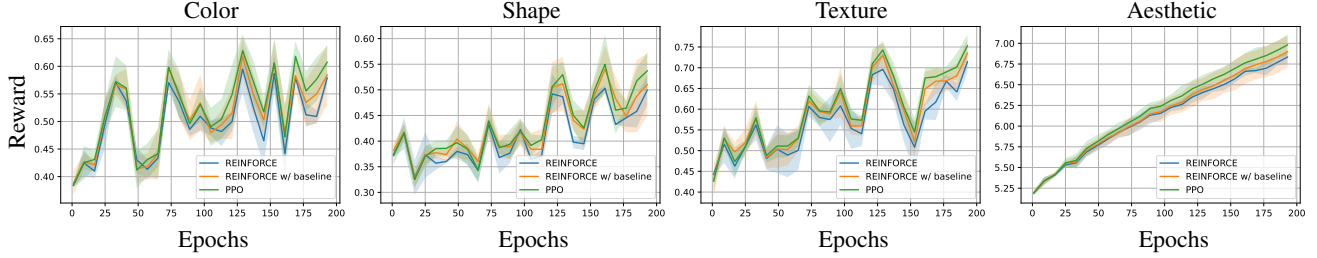


Figure 2. Evaluating REINFORCE vs. PPO trade-off by comparing: REINFORCE (Eq. 8), REINFORCE with baseline correction term (Eq. 9), and PPO (Eq. 6). We evaluate on the T2I-CompBench benchmark over three image attributes: Color, Shape, and Texture. We also compare on the aesthetic task. Y-axis corresponds to the training reward, x-axis corresponds to the training epoch. Results are averaged over 3 runs; shaded areas indicate 80% prediction intervals.

being unbiased in expectation (Gupta et al., 2024a; Mohamed et al., 2020). A simple choice of baseline correction can be the average reward across the K trajectories, i.e.:

$$b^i = \frac{1}{k} \sum_{i=0}^K r(\mathbf{x}_0^i). \quad (15)$$

However, we choose the leave-one-out average baseline, with average taken across all samples in the trajectory, except the current sample i , i.e.:

$$b^i = \frac{1}{k-1} \sum_{j \neq i} r(\mathbf{x}_0^j). \quad (16)$$

Originally RLOO sampling and baseline corrections were proposed in the context of REINFORCE, with a focus on on-policy optimization (Ahmadian et al., 2024; Kool et al., 2019), whereas we are applying these in the off-policy step of PPO. We call this method *leave-one-out PPO* (LOOP). Provenly, LOOP has lower variance than PPO:

Proposition 4.1. *The LOOP estimator $\hat{J}_\theta^{\text{LOOP}}(\pi)$ (Eq. 14) has lower variance than the PPO estimator $\hat{J}_\theta^{\text{PPO}}(\pi)$ (Eq. 13):*

$$\text{Var} \left[\hat{J}_\theta^{\text{LOOP}}(\pi) \right] < \text{Var} \left[\hat{J}_\theta^{\text{PPO}}(\pi) \right]. \quad (17)$$

Proof. Since the sampled trajectories are independent:

$$\text{Var} \left[\hat{J}_\theta^{\text{LOOP}}(\pi) \right] = \frac{1}{K^2} \text{Var} \left[\hat{J}_\theta^{\text{PPO}}(\pi) \right] < \text{Var} \left[\hat{J}_\theta^{\text{PPO}}(\pi) \right]. \quad \square$$

5. Experimental Setup

Benchmark. Text-to-image diffusion and language models often fail to satisfy an essential reasoning skill of attribute binding. Attribute binding reasoning capability refers to the ability of a model to generate images with attributes such as color, shape, texture, spatial alignment, (and others) specified in the input prompt. In other words, generated

images often fail to *bind* certain *attributes* specified in the instruction prompt (Huang et al., 2023; Ramesh et al., 2022; Fu & Cheng, 2024).

Since attribute binding seems to be a basic requirement for useful real-world applications, we choose the T2I-CompBench benchmark (Huang et al., 2023), which contains multiple attribute binding/image compositionality tasks, and its corresponding reward metric to benchmark text-to-image generative models. We also select two common tasks from RL for diffusion works: improving aesthetic quality of generation, and image-text semantic alignment (Black et al., 2023; Fan et al., 2024). To summarize, we choose the following tasks for the RL optimization: (i) Color, (ii) Shape, (iii) Texture, (iv) 2D Spatial, (v) Numeracy, (vi) Aesthetic, (vii) Image-text Alignment. For all tasks, the prompts are split into training/validation prompts. We report the average reward on both training and validation split.

Model. As the base diffusion model, we use Stable diffusion V2 (Rombach et al., 2022), which is a latent diffusion model. For optimization, we fully update the UNet model, with a learning rate of $1e^{-5}$. We also tried LORA fine-tuning (Hu et al., 2021), but the results were not satisfactory, so we update the entire model instead. The hyper-parameters are reported in Appendix A.

6. Results and Discussion

6.1. REINFORCE vs. PPO efficiency-effectiveness trade-off

We discuss our empirical results for the REINFORCE vs. PPO efficiency-effectiveness trade-off. Our empirical validation of the trade-off compares the following methods:

REINFORCE. The REINFORCE policy gradient for diffusion fine-tuning (Eq. 8).

REINFORCE with baseline correction. We compare the REINFORCE policy gradient with a baseline correction

Table 1. Comparing the performance of the proposed LOOP method with state-of-the-art baselines on the T2I-CompBench benchmark over image attributes such as Color, Shape, Texture, Spatial relation, and Numeracy. The metrics in this table are average reward on an unseen test set (higher is better). For each prompt we generate and average rewards across 10 different generated images.

Model	Color \uparrow	Shape \uparrow	Texture \uparrow	Spatial \uparrow	Numeracy \uparrow
Stable v1.4 (Rombach et al., 2022)	0.3765	0.3576	0.4156	0.1246	0.4461
Stable v2 (Rombach et al., 2022)	0.5065	0.4221	0.4922	0.1342	0.4579
Composable v2 (Liu et al., 2022)	0.4063	0.3299	0.3645	0.0800	0.4261
Structured v2 (Feng et al., 2022)	0.4990	0.4218	0.4900	0.1386	0.4550
Attn-Exct v2 (Chefer et al., 2023)	0.6400	0.4517	0.5963	0.1455	0.4767
GORS unbiased (Huang et al., 2023)	0.6414	0.4546	0.6025	0.1725	–
GORS (Huang et al., 2023)	0.6603	0.4785	0.6287	0.1815	0.4841
PPO (Black et al., 2023)	0.6821	0.5655	0.6909	0.1961	0.5102
LOOP ($k = 2$)	0.6785	0.5746	0.6937	0.1800	0.5072
LOOP ($k = 3$)	0.7515	0.6220	0.7353	0.1966	0.5242
LOOP ($k = 4$)	0.7859	0.6676	0.7518	0.2136	0.5422

Table 2. Comparing REINFORCE with PPO on the T2I-CompBench benchmark over three image attributes: Color, Shape, and Texture. The metrics in this table are average reward on an unseen test set (higher is better). For each prompt, average rewards over 10 independent generated images are calculated.

Method	Color \uparrow	Shape \uparrow	Texture \uparrow
REINFORCE	0.6438	0.5330	0.6359
REINFORCE w/ BC	0.6351	0.5347	0.6656
PPO	0.6821	0.5655	0.6909

(BC) term (Eq. 9). For the baseline term, we choose the average reward for the given prompt (Black et al., 2023).

PPO. The PPO objective for diffusion fine-tuning with importance sampling and clipping (Eq. 6).

Figure 2 shows the training reward over epochs for the attributes: Color, Shape, and Texture from the T2I-CompBench benchmark, and training reward from optimizing the aesthetic model. It is clear that REINFORCE policy gradient is not effective in terms of performance, as compared to other variants. Adding a baseline correction term indeed improves the training performance, validating the effectiveness of baseline in terms of training performance, possibly because of reduced variance. PPO achieves the highest training reward, validating the effectiveness of importance sampling and clipping for diffusion fine-tuning.

We also evaluate the performance on a separate validation set. For each validation prompt, we generate 10 independent images from the diffusion policy, and average the reward, finally averaging over all evaluation prompts. The validation results are reported in Table 2. The results are consistent with the pattern observed with the training rewards, i.e., REINFORCE with baseline provides a better performance than plain REINFORCE, suggesting that baseline correction

Table 3. Comparing the performance of LOOP with PPO on the aesthetic and image-text alignment tasks. Higher values are better.

Method	Aesthetic \uparrow	Image Align. \uparrow
PPO (Black et al., 2023)	6.8135	20.466
LOOP ($k = 2$)	6.8617	20.788
LOOP ($k = 3$)	7.0772	20.619
LOOP ($k = 4$)	7.8606	20.909

indeed helps with the final performance. Nevertheless, PPO still performs better than REINFORCE.

We now have empirical evidence supporting the *efficiency-effectiveness trade-off* discussed in Section 3. From these results, we can conclude that fine-tuning text-to-image diffusion models is more effective with IS and clipping from PPO, or baseline corrections from REINFORCE. This bolsters our motivation for proposing LOOP as an approach to effectively combine these methods.

6.2. Evaluating LOOP

Next we discuss the results from our proposed RL for diffusion fine-tuning method, LOOP.

Performance during training. Figure 3 shows the training reward curves for different tasks, against number of epochs. LOOP outperforms PPO across all seven tasks consistently throughout training. This establishes the effectiveness of sampling multiple diffusion trajectories per input prompt, and the leave-one-out baseline correction term (Eq. 10) during training. Training reward curve is smoother for the aesthetic task, as compared to tasks from the T2I-CompBench benchmark. We hypothesise that improving the attribute binding property of diffusion model is a harder task than improving the aesthetic quality of generated images.

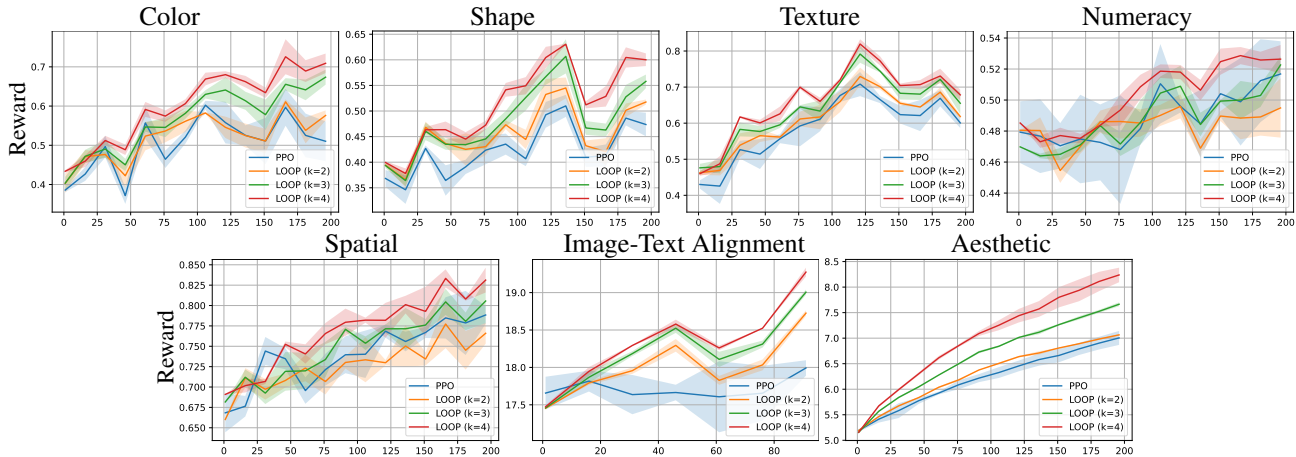


Figure 3. Comparing PPO with proposed LOOP on the T2I-CompBench benchmark w.r.t. image attributes: Color, Shape, Texture, Numeracy, and Spatial relationship. We also compare against aesthetic and image-text alignment tasks (Black et al., 2023). The y-axis corresponds to the training reward; the x-axis corresponds to the training epoch. Results are averaged over 3 independent training runs; shaded areas indicate 80% prediction intervals.

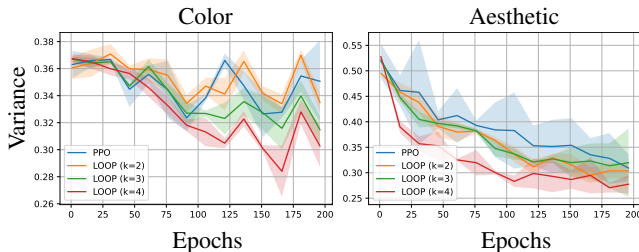


Figure 4. Training reward variance for the color, and aesthetic task. The y-axis corresponds to the training reward variance; the x-axis corresponds to the training epoch. Results are averaged over 3 runs; shaded areas indicate 80% prediction intervals. We observe that higher values of samples reused (i.e., k) produce lower reward variance during training.

Table 1 reports the validation rewards across different tasks from the T2I-CompBench benchmark. LOOP outperforms PPO and other strong supervised learning based baseline significantly across all tasks. It shows that PPO improves the attribute-binding reasoning ability of the diffusion model compared to other supervised learning based methods.

For the aesthetic and image-text alignment objectives, the validation rewards are reported in Table 3. LOOP results in a **15.37%** relative improvement over PPO for the aesthetic task, and a **2.16%** improvement over PPO for the image-text alignment task.

Impact of number of independent trajectories (k). The LOOP variant with number of independent trajectories $K = 4$ performs the best across all tasks, followed by the variant $K = 3$. This is intuitive given that Monte-Carlo estimates get better with more number of samples (Owen, 2013). Surprisingly, the performance of the variant with $K = 2$ is comparable to PPO.

Impact on training variance. We evaluate whether LOOP results in a lower empirical variance than PPO, as proved

theoretically in Lemma 4.1. Figure 4 reports the empirical reward variance during training for the color attribute and aesthetic objective. LOOP results in a lower empirical variance than PPO, thereby empirically validating our claim that LOOP has lower variance than PPO.

Qualitative results. For a qualitative evaluation of the attribute-binding reasoning ability, we present some example image generations from SD, PPO, and LOOP in Figure 1. In the first example, the input prompt specifies a black colored ball with a white cat. Stable diffusion (SD) and PPO fail to bind the color black with the generated ball, whereas LOOP successfully binds that attribute. Similarly, in the third example, SD and PPO fail to bind the hexagon shape attribute to the watermelon, whereas LOOP manages to do that. In the fourth example, SD and PPO fail to add the horse object itself, whereas LOOP adds the horse with the specified black color, and flowing cyan patterns.

7. Conclusion

We have studied the **efficiency-effectiveness** trade-off between two fundamental RL for diffusion methods: REINFORCE, and PPO. REINFORCE, while computationally efficient and easier to implement, is subpar to PPO in terms of sample efficiency and performance. Building on these insights, we have introduced a simple and effective RL for diffusion method, LOOP, which builds on the variance reduction techniques from REINFORCE and the effectiveness and robustness of PPO. We have found that LOOP improves over diffusion models on multiple black-box objectives. A limitation of LOOP is that sampling multiple diffusion trajectories per prompt can lead to more computational overhead and an increase in training time. A potential future direction would be to keep the effectiveness of LOOP while maintaining the computational complexity of PPO.

Impact Statement

This paper presents work whose goal is to advance the field of Machine Learning. There are many potential societal consequences of our work, none which we feel must be specifically highlighted here.

References

- Achiam, J., Held, D., Tamar, A., and Abbeel, P. Constrained policy optimization. In *International conference on machine learning*, pp. 22–31. PMLR, 2017.
- Ahmadian, A., Cremer, C., Gallé, M., Fadaee, M., Kretzner, J., Pietquin, O., Üstün, A., and Hooker, S. Back to basics: Revisiting REINFORCE style optimization for learning from human feedback in LLMs. *arXiv preprint arXiv:2402.14740*, 2024.
- Austin, J., Johnson, D. D., Ho, J., Tarlow, D., and Van Den Berg, R. Structured denoising diffusion models in discrete state-spaces. *Advances in Neural Information Processing Systems*, 34:17981–17993, 2021.
- Black, K., Janner, M., Du, Y., Kostrikov, I., and Levine, S. Training diffusion models with reinforcement learning. *arXiv preprint arXiv:2305.13301*, 2023.
- Blattmann, A., Rombach, R., Ling, H., Dockhorn, T., Kim, S. W., Fidler, S., and Kreis, K. Align your latents: High-resolution video synthesis with latent diffusion models. In *Proceedings of the IEEE/CVF Conference on Computer Vision and Pattern Recognition*, pp. 22563–22575, 2023.
- Chefer, H., Alaluf, Y., Vinker, Y., Wolf, L., and Cohen-Or, D. Attend-and-excite: Attention-based semantic guidance for text-to-image diffusion models. *ACM Transactions on Graphics (TOG)*, 42(4):1–10, 2023.
- Chen, Kevin, Cusumano-Towner, Marco, Huval, Brody, Petrenko, Aleksei, Hamburger, Jackson, Koltun, Vladlen, and Krähenbühl, Philipp. Reinforcement Learning for Long-Horizon Interactive LLM Agents. *arXiv preprint arXiv:2502.01600*, 2025.
- Engstrom, L., Ilyas, A., Santurkar, S., Tsipras, D., Janoos, F., Rudolph, L., and Madry, A. Implementation matters in deep RL: A case study on ppo and trpo. In *International conference on learning representations*, 2019.
- Fan, Y., Watkins, O., Du, Y., Liu, H., Ryu, M., Boutilier, C., Abbeel, P., Ghavamzadeh, M., Lee, K., and Lee, K. Reinforcement learning for fine-tuning text-to-image diffusion models. *Advances in Neural Information Processing Systems*, 36, 2024.
- Feng, W., He, X., Fu, T.-J., Jampani, V., Akula, A., Narayana, P., Basu, S., Wang, X. E., and Wang, W. Y. Training-free structured diffusion guidance for compositional text-to-image synthesis. *arXiv preprint arXiv:2212.05032*, 2022.
- Fu, H. and Cheng, G. Enhancing semantic mapping in text-to-image diffusion via gather-and-bind. *Computers & Graphics*, 125:104118, 2024.
- Greensmith, E., Bartlett, P. L., and Baxter, J. Variance reduction techniques for gradient estimates in reinforcement learning. *Journal of Machine Learning Research*, 5(9), 2004.
- Gu, Y., Wang, Z., Yin, Y., Xie, Y., and Zhou, M. Diffusion-RPO: Aligning diffusion models through relative preference optimization. *arXiv preprint arXiv:2406.06382*, 2024.
- Gupta, S., Jeunen, O., Oosterhuis, H., and de Rijke, M. Optimal baseline corrections for off-policy contextual bandits. In *Proceedings of the 18th ACM Conference on Recommender Systems*, pp. 722–732, 2024a.
- Gupta, S., Oosterhuis, H., and de Rijke, M. Practical and robust safety guarantees for advanced counterfactual learning to rank. In *Proceedings of the 33rd ACM International Conference on Information and Knowledge Management*, pp. 737–747, 2024b.
- Ho, J., Jain, A., and Abbeel, P. Denoising diffusion probabilistic models. *Advances in neural information processing systems*, 33:6840–6851, 2020.
- Hu, E. J., Shen, Y., Wallis, P., Allen-Zhu, Z., Li, Y., Wang, S., Wang, L., and Chen, W. LORA: Low-rank adaptation of large language models. *arXiv preprint arXiv:2106.09685*, 2021.
- Huang, K., Sun, K., Xie, E., Li, Z., and Liu, X. T2I-CompBench: A comprehensive benchmark for open-world compositional text-to-image generation. *Advances in Neural Information Processing Systems*, 36:78723–78747, 2023.
- Huang, S., Noukhovitch, M., Hosseini, A., Rasul, K., Wang, W., and Tunstall, L. The N+ implementation details of RLHF with PPO: A case study on TL; DR summarization. *arXiv preprint arXiv:2403.17031*, 2024.
- Kool, W., van Hoof, H., and Welling, M. Buy 4 REINFORCE samples, get a baseline for free! 2019.
- Lee, K., Liu, H., Ryu, M., Watkins, O., Du, Y., Boutilier, C., Abbeel, P., Ghavamzadeh, M., and Gu, S. S. Aligning text-to-image models using human feedback. *arXiv preprint arXiv:2302.12192*, 2023.

- Li, S., Kallidromitis, K., Gokul, A., Kato, Y., and Kozuka, K. Aligning diffusion models by optimizing human utility. *arXiv preprint arXiv:2404.04465*, 2024.
- Liu, N., Li, S., Du, Y., Torralba, A., and Tenenbaum, J. B. Compositional visual generation with composable diffusion models. In *European Conference on Computer Vision*, pp. 423–439. Springer, 2022.
- Loshchilov, I. and Hutter, F. Decoupled weight decay regularization. In *International Conference on Learning Representations*, 2017. URL <https://arxiv.org/abs/1711.05101>.
- Mohamed, S., Rosca, M., Figurnov, M., and Mnih, A. Monte Carlo gradient estimation in machine learning. *Journal of Machine Learning Research*, 21(132):1–62, 2020.
- Owen, A. B. *Monte Carlo theory, methods and examples*. <https://artowen.su.domains/mc/>, 2013.
- Queeney, J., Paschalidis, Y., and Cassandras, C. G. Generalized proximal policy optimization with sample reuse. *Advances in Neural Information Processing Systems*, 34: 11909–11919, 2021.
- Rafailov, R., Sharma, A., Mitchell, E., Manning, C. D., Ermon, S., and Finn, C. Direct preference optimization: Your language model is secretly a reward model. *Advances in Neural Information Processing Systems*, 36, 2024.
- Ramesh, A., Dhariwal, P., Nichol, A., Chu, C., and Chen, M. Hierarchical text-conditional image generation with clip latents. *arXiv preprint arXiv:2204.06125*, 1(2):3, 2022.
- Rombach, R., Blattmann, A., Lorenz, D., Esser, P., and Ommer, B. High-resolution image synthesis with latent diffusion models. In *Proceedings of the IEEE/CVF conference on computer vision and pattern recognition*, pp. 10684–10695, 2022.
- Schuhmann, C., Beaumont, R., Vencu, R., Gordon, C., Wightman, R., Cherti, M., Coombes, T., Katta, A., Mullis, C., Wortsman, M., et al. Laion-5b: An open large-scale dataset for training next generation image-text models. *Advances in Neural Information Processing Systems*, 35: 25278–25294, 2022.
- Schulman, J. Trust region policy optimization. *arXiv preprint arXiv:1502.05477*, 2015.
- Schulman, J., Wolski, F., Dhariwal, P., Radford, A., and Klimov, O. Proximal policy optimization algorithms. *arXiv preprint arXiv:1707.06347*, 2017.
- Sohl-Dickstein, J., Weiss, E., Maheswaranathan, N., and Ganguli, S. Deep unsupervised learning using nonequilibrium thermodynamics. In *International conference on machine learning*, pp. 2256–2265. PMLR, 2015.
- Sutton, R. S. and Barto, A. G. *Reinforcement learning: An introduction*. The MIT Press, 2018.
- Swaminathan, A. and Joachims, T. The self-normalized estimator for counterfactual learning. In *Advances in Neural Information Processing Systems*, volume 28, 2015.
- Wallace, B., Dang, M., Rafailov, R., Zhou, L., Lou, A., Purushwalkam, S., Ermon, S., Xiong, C., Joty, S., and Naik, N. Diffusion model alignment using direct preference optimization. In *Proceedings of the IEEE/CVF Conference on Computer Vision and Pattern Recognition*, pp. 8228–8238, 2024.
- Wang, C., Uehara, M., He, Y., Wang, A., Biancalani, T., Lal, A., Jaakkola, T., Levine, S., Wang, H., and Regev, A. Fine-tuning discrete diffusion models via reward optimization with applications to dna and protein design. *arXiv preprint arXiv:2410.13643*, 2024.
- Williams, R. J. Simple statistical gradient-following algorithms for connectionist reinforcement learning. *Machine Learning*, 8:229–256, 1992.
- Xie, Z., Yu, C., and Qiao, W. Dropout strategy in reinforcement learning: Limiting the surrogate objective variance in policy optimization methods. *arXiv preprint arXiv:2310.20380*, 2023.
- Xu, J., Liu, X., Wu, Y., Tong, Y., Li, Q., Ding, M., Tang, J., and Dong, Y. Imagereward: Learning and evaluating human preferences for text-to-image generation. *Advances in Neural Information Processing Systems*, 36, 2024.
- Xu, M., Powers, A. S., Dror, R. O., Ermon, S., and Leskovec, J. Geometric latent diffusion models for 3D molecule generation. In *International Conference on Machine Learning*, pp. 38592–38610. PMLR, 2023.
- Yang, Shentao, Chen, Tianqi, and Zhou, Mingyuan. A Dense Reward View on Aligning Text-to-Image Diffusion with Preference. In *International Conference on Machine Learning*, pages 55998–56032. PMLR, 2024.
- Zeng, Y., Liu, G., Ma, W., Yang, N., Zhang, H., and Wang, J. Token-level direct preference optimization. *arXiv preprint arXiv:2404.11999*, 2024.
- Zheng, R., Dou, S., Gao, S., Hua, Y., Shen, W., Wang, B., Liu, Y., Jin, S., Zhou, Y., Xiong, L., et al. Delve into PPO: Implementation matters for stable RLHF. In *NeurIPS 2023 Workshop on Instruction Tuning and Instruction Following*, 2023.

Zhong, H., Feng, G., Xiong, W., Cheng, X., Zhao, L., He, D.,
Bian, J., and Wang, L. DPO meets PPO: Reinforced token
optimization for RLHF. *arXiv preprint arXiv:2404.18922*,
2024.

A. Hyperparameter and Implementation Details

For REINFORCE (including REINFORCE with baseline correction term), PPO, and LOOP the number of denoising steps (T) is set to 50. The diffusion guidance weight is set to 5.0. For optimization, we use AdamW (Loshchilov & Hutter, 2017) with a learning rate of $1e^{-5}$, and the weight decay of $1e^{-4}$, with other parameters kept at the default value. We clip the gradient norm to 1.0. We train all models using 8 A100 GPUs with a batch size of 4 per GPU. The clipping parameter ϵ for PPO, and LOOP is set to $1e^{-4}$.

B. Additional Qualitative Examples

We present some additional qualitative examples in this section.

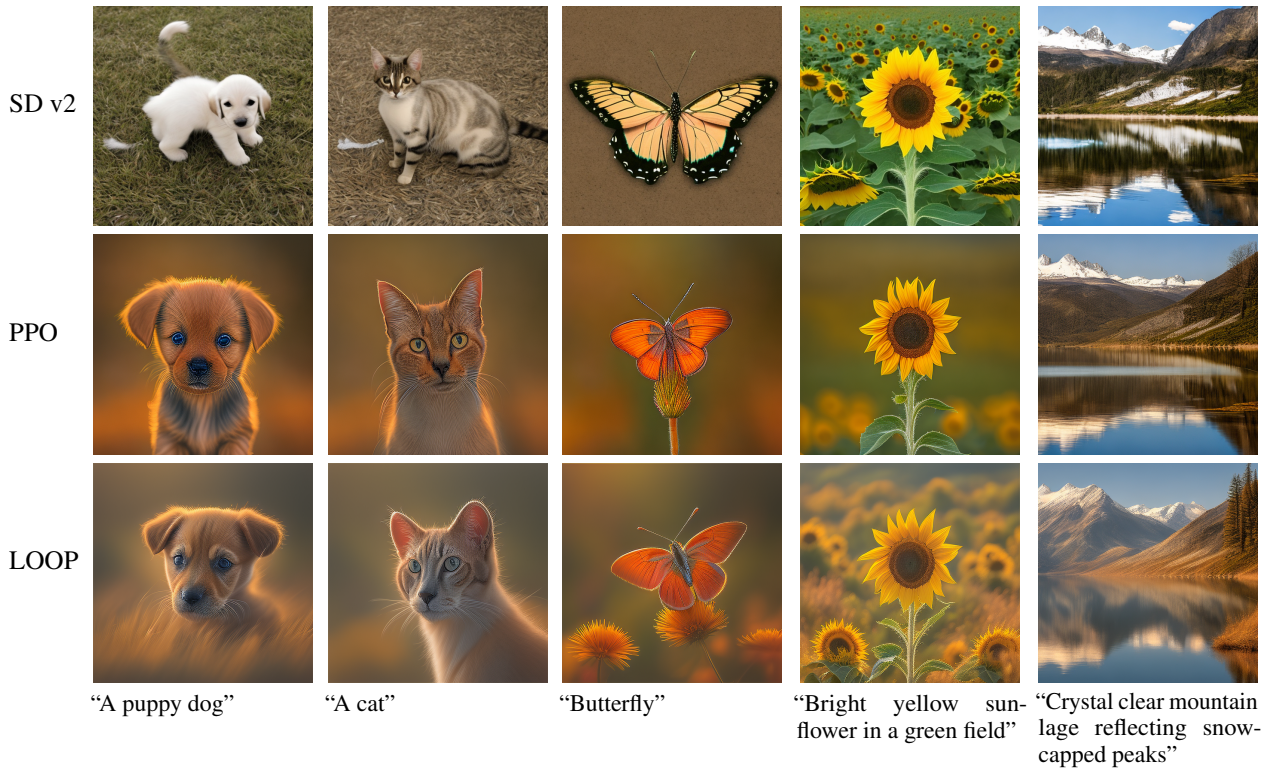


Figure 5. **LOOP improves aesthetic quality.** Qualitative examples are presented from images generated via: Stable Diffusion 2.0 (first row), PPO (second row), and LOOP $k = 4$ (third row). LOOP consistently generates more aesthetic images, as compared to PPO and SD.



Figure 6. Additional qualitative examples presented from images generated via Stable Diffusion 2.0 (first row), PPO (second row), and LOOP $k = 4$ (third row). LOOP consistently generates more aesthetic images, as compared to PPO and SD (first, third, and fifth prompt). LOOP also binds the color attribute (teal branch in second example, and pink cornfield in the forth example), where SD and PPO fail.